ISSN 1674-1056
http://cpb.iphy.ac.cn
http://iopscience.iop.org/cpb
中国物理 B
Chinese Physics
中国物理
Chinese Physics B

Flowrate behavior and clustering of self-driven robots in a channel

Bo Tian(田波), Wang-Ping Sun(孙王平), Ming Li(李明), Rui Jiang(姜锐), Mao-Bin Hu(胡茂彬)
Citation: Chin. Phys. B . 2018, 27(3): 038902. **doi:** 10.1088/1674-1056/27/3/038902

Journal homepage: http://cpb.iphy.ac.cn; http://iopscience.iop.org/cpb

What follows is a list of articles you may be interested in

A uniform framework of projection and community detection for one-mode network in bipartite networks

Guolin Wu(吴果林), Changgui Gu(顾长贵), Lu Qiu(邱路), Huijie Yang(杨会杰)
Chin. Phys. B . 2017, 26(12): 128901. **doi:** 10.1088/1674-1056/26/12/128901

Collective motion of active particles in environmental noise

Qiu-shi Chen(陈秋实), Ming Ji(季铭)
Chin. Phys. B . 2017, 26(9): 098903. **doi:** 10.1088/1674-1056/26/9/098903

Feedback arcs and node hierarchy in directed networks

Jin-Hua Zhao(赵金华), Hai-Jun Zhou(周海军)
Chin. Phys. B . 2017, 26(7): 078901. **doi:** 10.1088/1674-1056/26/7/078901

Scaling of weighted spectral distribution in weighted small-world networks

Bo Jiao(焦波), Xiao-Qun Wu(吴晓群)
Chin. Phys. B . 2017, 26(2): 028901. **doi:** 10.1088/1674-1056/26/2/028901

Community detection in signed networks based on discrete-time model

Jianrui Chen(陈建芮), Li Zhang(张莉), Weiwei Liu(刘维维), Zaizai Yan(闫在在)
Chin. Phys. B . 2017, 26(1): 018901. **doi:** 10.1088/1674-1056/26/1/018901

Flowrate behavior and clustering of self-driven robots in a channel*

Bo Tian(田波)[1,2], Wang-Ping Sun(孙王平)[1], Ming Li(李明)[1,†], Rui Jiang(姜锐)[3], and Mao-Bin Hu(胡茂彬)[1,‡]

[1] *School of Engineering Science, University of Science and Technology of China, Hefei* 230026, *China*
[2] *School of Engineering, Anhui Agricultural University, Hefei* 230036, *China*
[3] *MOE Key Laboratory for Urban Transportation Complex Systems Theory and Technology, Beijing Jiaotong University, Beijing* 100044, *China*

(Received 11 October 2017; revised manuscript received 12 December 2017; published online 11 February 2018)

In this paper, the collective motion of self-driven robots is studied experimentally and theoretically. In the channel, the flowrate of robots increases with the density linearly, even if the density of the robots tends to 1.0. There is no abrupt drop in the flowrate, similar to the collective motion of ants. We find that the robots will adjust their velocities by a serial of tiny collisions. The speed-adjustment will affect both robots involved in the collision, and will help to maintain a nearly uniform velocity for the robots. As a result, the flowrate drop will disappear. In the motion, the robots neither gather together nor scatter completely. Instead, they form some clusters to move together. These clusters are not stable during the moving process, but their sizes follow a power-law-alike distribution. We propose a theoretical model to simulate this collective motion process, which can reproduce these behaviors well. Analytic results about the flowrate behavior are also consistent with experiments.

Keywords: self-driven robots, collective motion, flowrate, clustering

PACS: 89.75.Fb, 45.70.Vn, 87.23.Cc **DOI:** 10.1088/1674-1056/27/3/038902

1. Introduction

Collective motion is a common phenomenon existing in both nature and human society. It can be observed in various natural contexts, including fish schools,[1–3] sheep herds,[4] bird flocks,[5] insect swarms,[6,7] bacterial colonies,[8–10] cells,[11] as well as nonliving active systems.[12–14] Collective movement can also be found in many human activities, such as the vehicular traffic flow and the pedestrian flow.[15–21] From the coordinated motion of insects as small as ants to large mammals like humans, the study of collective motion shows the emergence of rich dynamical behaviors and patterns.

Generally, collective movement must occur in a system containing a large number of individuals, which can move coordinately and orderly. Since the statistical mechanics is an effective tool to deal with large populations, many efforts have been devoted to understand the mechanism of collective movement in the perspective of statistical physics.[22,23] These studies demonstrate that some long-ranged nematic orders of motion can emerge from simple microcosmic and local mechanisms. This indicates that the individuals do not need to know the information of the whole system to keep a complex collective movement.

One of the collective movements attracting a lot of attention is the motion of the self-propelled agents along a one-dimensional trial or channel, such as the motion of ants[7,24–26] and the traffic flow.[27–31] However, the motion of ants and the traffic flow are very different from each other. John *et al*. studied the ant traffic on trails and found that there is no jammed phase (or flowrate drop) in this system.[26] A similar phenomenon can also be found in the swarming movement of camphor boats in a ring channel.[32,33] On the other hand, traffic jam is a common phenomenon of our daily lives. Some studies suggest that the ants' reaction to the pheromone of previous ants is a key factor for the absence of jammed phase.[34] From a traffic point of view, the collective motion of ants shows a self-organization structure with maximal efficiency,[35,36] similar to the spontaneous formation of lanes in bidirectional pedestrian flow.[37,38]

In this paper, we show that the absence of flowrate drop phenomenon can also be observed in the system of self-propelled robots. In particular, the self-propelled robots considered here do not have any intelligent reaction or pheromone, which are different from the ants. We find that the robots tend to form some clusters to move together. To better understand the phenomenon, we also propose a simple robot-following model to reproduce the behavior.

2. Experiment results

The devices used in our experiment are toy robots called Hexbug Nano, as shown in Fig. 1(a). The motion of this robot

*Project supported by the Key Research and Development Program, China (Grant No. 2016YFC0802508) and the National Natural Science Foundation of China (Grant Nos. 11672289 and 11422221).

†Corresponding author. E-mail: minglichn@ustc.edu.cn
‡Corresponding author. E-mail: humaobin@ustc.edu.cn

© 2018 Chinese Physical Society and IOP Publishing Ltd

relies on a vibration motor, which is powered by a 1.5 V button battery. When the vibration motor is turned on, the robot will move forward by shaking its 12 flexible legs on both sides. These Hexbugs have been used to study the collective motion of randomly moving robots, generating directed movement of asymmetric gears.[39] Due to the self-propelling property and the easy controllability, the Hexbugs system is proved to be a good example of studying the collective motions of robots. For detailed information about the robots, one can refer to Refs. [39] and [40].

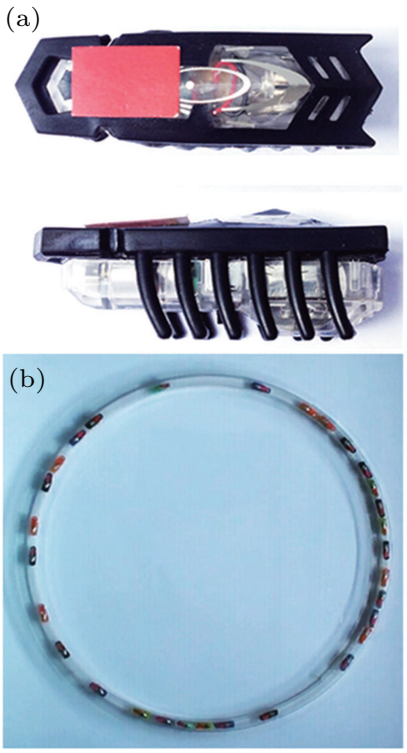


Fig. 1. (color online) (a) Top and side views of the robot used in the experiment. The size of the robot is 43 mm×12 mm×15 mm. (b) A snapshot of the experiment with thirty robots.

In this paper, we focus on the movement and clustering behaviors of the robots running in a circular track as shown in Fig. 1(b). The interior width and height of the track are 20 mm, which is slightly larger than the width of the robot. The diameter of the circular track is 800 mm. The maximum number of the robots in the track, i.e., the capacity of the track, is $N_{\max} = 55$. At the beginning of each experiment, the robots are put in the track evenly. The robots can move along the track and the overtaking is prevented. In order to stabilize the power output, each battery is used for no more than 20 min. The first 10 min of an experiment is regarded as the transient state. Then, we collect the movement characteristics of the robots in the following 10 min. A video camera is adopted to capture the movement of the robots. In the afterward video-processing, the track is divided into 55 pieces to label the position of the robots, since the capacity of the track is $N_{\max} = 55$ robots, as shown in Fig. 2.

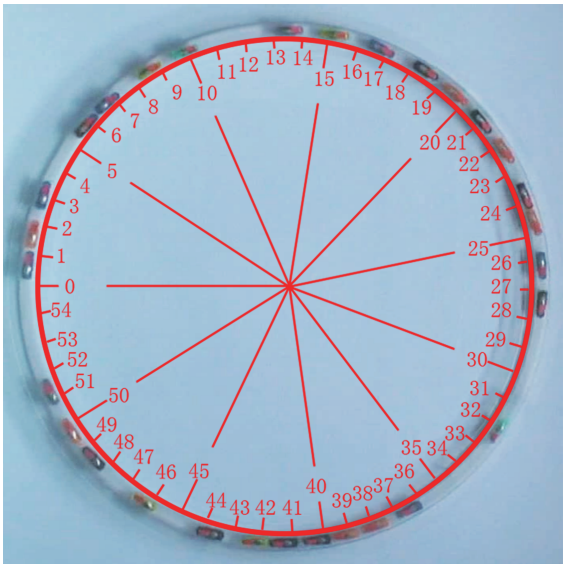


Fig. 2. (color online) Snapshot of the track used in the experiment. The capacity of the track is $N_{\max} = 55$ robots. We divide the track into 55 pieces (indicated by red). In the experiment, we use these scales to label the position of the robots.

We first consider the flow–density relation in this system. Figure 3 shows the relationship between the average flow rate J with robot density ρ. Here, the density ρ is the ratio of the number of robots in the system to the capacity $N_{\max}$. One can see that the flow rate almost linearly increases with the density, and reaches the maximum at $\rho \to 1$. In other words, the velocity of the robot is relatively independent of the robot density, even if there can be multi-collisions between neighboring robots. The flowrate drop phenomenon does not appear in the system. This behavior is different from the vehicular traffic system, but similar to the ant flow.[26]

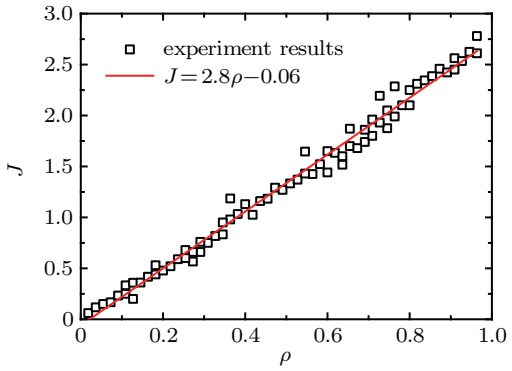


Fig. 3. (color online) Flow rate J plotted as a function of the density ρ. The scattered points are the experiment results and the red solid line is the fitting curve.

The vanishing of flowrate drop can be explained as follows. When the neighboring robots meet and collide, both robots will adjust their velocities slightly, but will not come to a motionless state. In particular, the previous robot will accelerate and the following robot will decelerate. As a result, both robots will come to similar velocities. This process occurs in a very short time even when there is a high density of

robots. The robots can move forward after the contact, and no stopping develops in the system. This situation can also be observed in the ant traffic. However, in the vehicular traffic flow, the vehicles will probably stop when they are close to each other. The vehicles also need more time to accelerate due to the slow-start mechanism. Therefore, flowrate drop will emerge in the vehicular traffic systems.

We also obtain the spacial–temporal (s–t) diagrams for low, intermediate, and high densities from the experiment, as shown in Fig. 4. We can see that for any densities, the s–t diagrams show the patterns with almost the same slope for the trajectory of each robot. This also indicates that the average velocity of the robot is independent of the density even when there are collisions between adjacent robots. The robots tend to form some clusters to move together. In the moving process, although some fluctuation may break the clusters accidentally, no cluster of zero velocity robots can be formed in the system. This clustering behavior is also observed in the ant flow system.[26,35,36] The dynamics of clustering is an interesting topic in the field of collective motion. For the robot system considered in this paper, the main difference lies in that there is no intelligence or pheromone of the self-propelled robots in the system.

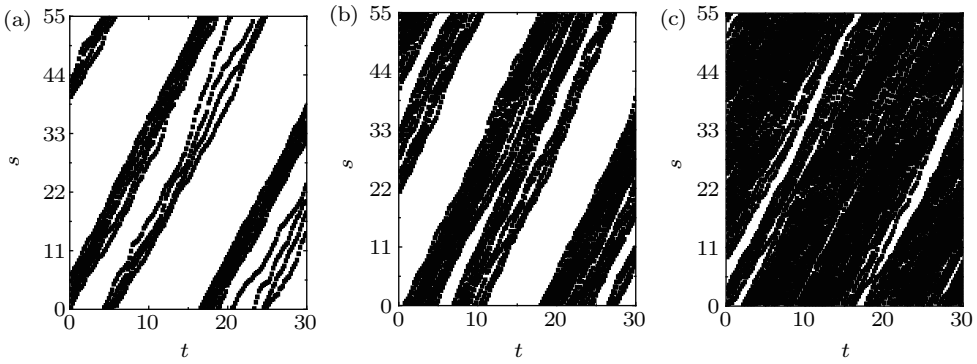


Fig. 4. The space–time diagrams for robots of low, intermediate, and high densities: (a) 10 robots ($\rho = 0.182$), (b) 20 robots ($\rho = 0.364$), (c) 40 robots ($\rho = 0.727$).

To characterize the clustering behavior, we further investigate the distribution of the cluster sizes in the motion of robots. Figure 5 shows the cluster–size distribution for different robot numbers obtained by experiments. One can see that the cluster size follows a power-law alike distribution. While there are some large clusters, most of the clusters only contain one or two robots. With more robots in the system, larger clusters will appear more frequently.

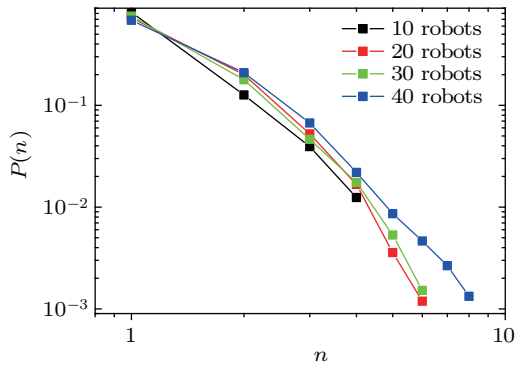


Fig. 5. (color online) Cluster-size distribution $P(n)$ for different numbers of robots. A cluster is defined as a serial of robots in which each pair of neighboring robots is separated by less than 5% body length. And the cluster sizes are obtained every 5 s.

3. Analysis and simulations

Now we consider the modeling and analysis of such a robot system. In the experiments, the robots are confined to a circular, narrow channel, in which overtaking and U-turn are not allowed. Similar to the molecular dynamics simulation, in our model the movement of robots is determined by

$$m\frac{\mathrm{d}^2x_i}{\mathrm{d}t^2} = F_i + \eta_i - \mu\frac{\mathrm{d}x_i}{\mathrm{d}t} + k(\Delta x_i^- - \Delta x_i^+), \qquad (1)$$

where m and x_i are the mass and position of robot i; F_i is the self-driven force of robot i, which takes the same value $F_i = F$ for each robot; η_i is the stochastic noise of the self-driven force for robot i, which could be different for the robots and also vary with time; and μ is the friction coefficient between the robots and the track (we assume a viscosity-alike form of friction). The fourth term on the right side of this equation is the interaction between robot i and the ones in the front and the back. When two adjacent robots meet and contact, there will be collisions that lead to the adjustment of both robots' acceleration and velocity. Here, we simply express this interaction by Hooke's law. Therefore, k is the elastic coefficient, and Δx_i^+ and Δx_i^- are the overlaps between robot i and the ones in the front and the back. This collision model can be regarded as a simplified version of the discrete element model (DEM) of granular particle interactions.

3.1. Analytical solution

For the convenience of mathematical processing, we rewrite Eq. (1) as

$$m\frac{\mathrm{d}v_i}{\mathrm{d}t} = F_i + \eta_i - \mu v_i + k(\Delta x_i^- - \Delta x_i^+), \tag{2}$$

where $v_i = \mathrm{d}x_i/\mathrm{d}t$ is used. One can average Eq. (2) over all the robots to obtain the average velocity of all the robots. That is

$$m\frac{\mathrm{d}\langle v\rangle}{\mathrm{d}t} = F + \langle\eta\rangle - \mu\langle v\rangle + k\left(\langle\Delta x^-\rangle - \langle\Delta x^+\rangle\right). \tag{3}$$

In our model, η takes an uniform distribution lying in $[-f, f]$, thus $\langle\eta\rangle = 0$. In addition, it is also easy to know that $\langle\Delta x^-\rangle = \langle\Delta x^+\rangle$ for the whole system. Thus we obtain

$$m\frac{\mathrm{d}\langle v\rangle}{\mathrm{d}t} = F - \mu\langle v\rangle. \tag{4}$$

The solution is

$$\langle v\rangle = \frac{F}{\mu}(1 - \mathrm{e}^{-\frac{\mu}{m}t}). \tag{5}$$

Here, the initial velocity ($t = 0$) is assumed to be 0. From Eq. (5), the characteristic time scale for acceleration is $\tau \approx m/\mu$. For $t \to \infty$, this equation gives the average velocity of the robots in the steady state

$$\langle v\rangle = \frac{F}{\mu}. \tag{6}$$

One can see that the mean velocity only depends on the average driving force and the friction. In the case of fixed average driving force and friction, the mean velocity will be constant. Then the flow rate of the robots in the steady state should be

$$J = \langle v\rangle\rho = \frac{F\rho}{\mu}. \tag{7}$$

Thus we can see that the flow rate J shows a linear relation with the robot density ρ, which is in agreement with the experiment results.

The setting of the collision term is a key factor in the modeling,

$$F_\mathrm{c} = k(\Delta x_i^- - \Delta x_i^+). \tag{8}$$

When two adjacent robots meet and collide with each other, we can expect that the value of overlaps (Δx_i^- and Δx_i^+) is quite small. Although their velocities will be adjusted slightly, the velocity of the following robot will not reduce to zero. The collision will happen in a very short time and the robots will separate quickly. Therefore, the collisions will not affect the average velocity of the robots. On the contrary, the collisions will help to form a uniform velocity of the robots. Therefore, the flowrate drop will not emerge.

However, for the traffic flow, the velocity of the following vehicle will usually reduce to zero quickly when it is too close to the previous vehicle, while the previous vehicle will not be affected at all. In this case, the velocity difference of the two adjacent vehicles will be enlarged. Moreover, the acceleration of the following vehicle also takes much more time. All these factors will induce more fluctuations into the movement of the vehicular traffic flow, which will finally lead to flowrate drop.

3.2. Simulation results

In the simulation, we use Eq. (1) to obtain the acceleration and velocity for each robot at each time step. Then, all robots move to their new positions. The simulation parameters are set as follows: $F = 2.8$, $\eta_i \in [-0.5, 0.5]$, $\mu = 1.0$, $m = 1.0$, $k = 10^6$, and time step $\Delta t = 10^{-5}$. The length of the robot is $L = 1$. For comparative purposes, the system size is $N_{\max}L$.

We first consider a system with only one robot. As shown in Fig. 6, the velocity increases with time, and tends to a constant. The relaxation time is less than one second. This is consistent with Eq. (5). In Fig. 7, we show the flow rate J obtained by simulations as a function of the density ρ in the steady state. The flow rate increases with the density linearly, similar to the analysis and experiment results. This indicates that our model can reproduce the robots' flow correctly.

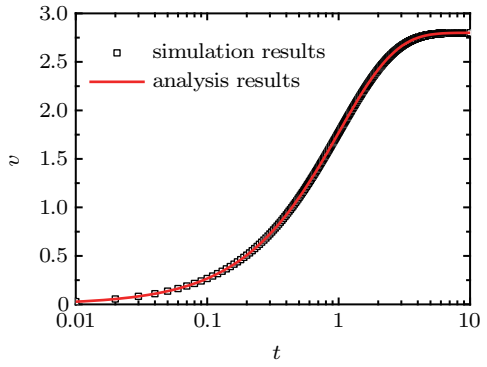


Fig. 6. (color online) The temporal evolution of the velocity for single robot. The scattered points are obtained by simulations and the solid line is the solution Eq. (5) for a single robot.

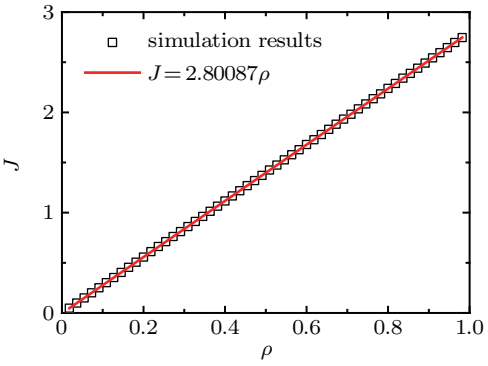


Fig. 7. (color online) Flow rate J plotted as a function of the density ρ. The scattered points are obtained by simulations and the red solid line is the fitting curve. The flow rate is obtained through the average of 100 realizations in every density.

The model discussed above is the deterministic model. This means that in the steady state all the robots form a stable configuration to move together. However, the experiment results shown in Fig. 4 reveal that although the average velocity is nearly invariable, the configuration of the robots could change over time. This is because that the self-driven forces

of the robots could change slightly for battery and mechanical reasons. To reflect this, we set that the stochastic noise η_i changes randomly with time. Specifically, in each time step, C robots are chosen randomly and their stochastic noise η_i will be reset with probability 0.1. Since the stochastic noise η_i is always chosen randomly from $[-0.5, 0.5]$, this resetting mechanism does not change the analysis results Eqs. (5) and (7).

In Fig. 8, we compare the space–time diagrams of simulations with different C ($C = 0, 1$) for different densities. One can see that with this force noise mechanism, the model can reproduce the experiments results very well. The robots form some clusters to move together, and the clusters break and restructure repeatedly. To feature this cluster forming process, we further give the simulation results of the size distribution of clusters in Fig. 9. We can find that the size follows a power-law alike distribution, similar to Fig. 5. With the increase of C, the forming of larger clusters becomes harder.

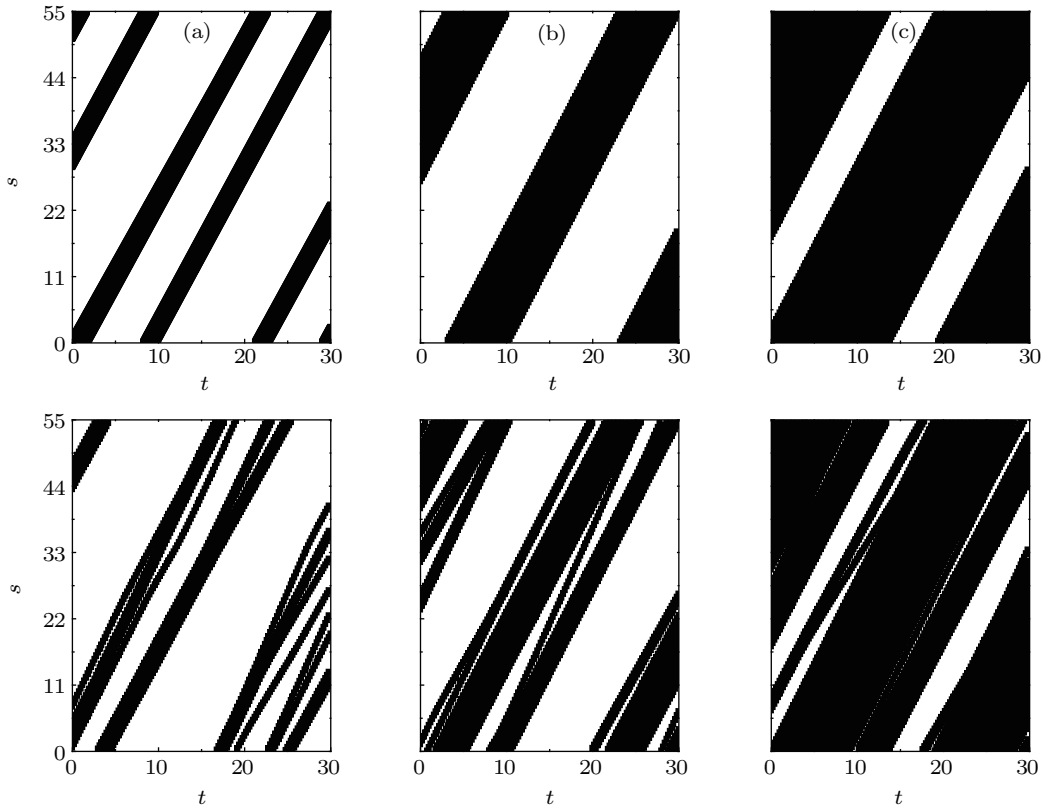


Fig. 8. The space–time diagrams from simulations. The number of robots that can change their stochastic noise is $C = 0$ (top row) and $C = 1$ (bottom row), respectively: (a) 10 robots ($\rho = 0.182$), (b) 20 robots ($\rho = 0.364$), (c) 40 robots ($\rho = 0.727$).

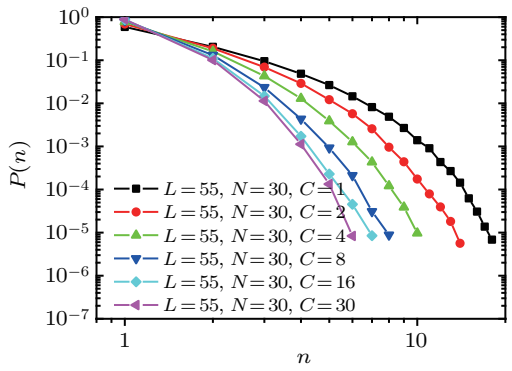


Fig. 9. (color online) Cluster-size distribution $P(n)$ for different numbers of robots that can change the stochastic noise C. The number of robots used in this simulation is $N = 30$.

4. Discussion and conclusion

In summary, we adopt the Hexbug robots to study the self-driven robots' collective motion in a circular channel system. We find that the flow rate changes linearly with the density, and there is no flowrate drop in the process. We propose a microscopic model to study the system's behavior. In this model, self propelling, stochastic noise, friction, and collision are all considered. The experiment results are well reproduced. By theoretical analysis of this model, we find that the tiny collisions between adjacent robots will help to maintain an uniform velocity for the robots, thus the traffic flowrate drop phenomenon will not emerge. We study the clustering behavior of this system. The robots neither gather together nor scatter completely. Instead, they form some clusters to move together. The size of the clusters follows a power-law-alike distribution. This distribution indicates that even if there are some giant clusters, small size clusters dominate in the system.

The findings suggest that the movement of such non-intelligent and non-pheromone self-driven robots is similar to the ant traffic, but it is different from the vehicle traffic. For

the robots or ants, when the neighboring individuals collide or meet each other, the contact will help to generate a similar speed for both individuals. Their velocities do not reduce to zero. This is the reason for the disappearance of flowrate drop phenomenon. In the future, we can expect that the collision-alike mechanism of Eq. (8) can be realized by advanced vehicle technologies without real collisions: the vehicle can detect the distances of vehicles in the front and the back, and then adjust its speed according to similar rules as Eq. (8). The outcome might lead to a smooth and non-jamming vehicular traffic flow, which will be meaningful for modern transportation systems.

References

[1] Vicsek T and Zafeiris A 2012 *Physics Reports* **517** 71
[2] Marchetti M C, Joanny J F, Ramaswamy S, Liverpool T B, Prost J, Rao M and Simha R A 2013 *Rev. Mod. Phys.* **85** 1143
[3] Gautrais J, Ginelli F, Fournier R, Blanco S, Soria M, Chaté H and Theraulaz G 2012 *PLoS Computational Biology* **8** e1002678
[4] Toulet S, Gautrais J, Bon R and Peruani F 2015 *PLoS One* **10** 1
[5] Bhattacharya K and Vicsek T 2010 *New J. Phys.* **12** 093019
[6] Romanczuk P, Couzin I D and Schimansky-Geier L 2009 *Phys. Rev. Lett.* **102** 010602
[7] Nishinari K, Chowdhury D and Schadschneider A 2003 *Phys. Rev. E* **67** 036120
[8] Ben-Jacob E, Cohen I and Levine H 2000 *Advances in Physics* **49** 395
[9] Yan G, Vertes P E, Towlson E K, Chew Y L, Walker D S, Schafer W R and Barabasi A L 2017 *Nature* **550** 519
[10] Chen L M 2016 *Acta Phys. Sin.* **65** 186401 (in Chinese)
[11] Rappel W J, Nicol A, Sarkissian A, Levine H and Loomis W F 1999 *Phys. Rev. Lett.* **83** 1247
[12] Weber C A, Hanke T, Deseigne J, Léonard S, Dauchot O, Frey E and Chaté H 2013 *Phys. Rev. Lett.* **110** 208001
[13] Lam K D N T, Schindler M and Dauchot O 2015 *New J. Phys.* **11** 113056
[14] Chen Q S and Ji Ming 2017 *Chin. Phys. B* **26** 098903
[15] Chowdhury D, Santen L and Schadschneider A 2000 *Physics Reports* **329** 199
[16] Sugiyama Y, Fukui M, Kikuchi M, Hasebe K, Nakayama A, Nishinari K, Tadaki S I and Yukawa S 2008 *New J. Phys.* **10** 033001
[17] Helbing D 2001 *Rev. Mod. Phys.* **73** 1067
[18] Schadschneider A, Chowdhury D and Nishinari K 2010 *Stochastic Transport in Complex Systems: from Molecules to Vehicles* (Elsevier)
[19] Qin Y Y, Wang H, Wang W and Wan Q 2017 *Acta Phys. Sin.* **66** 094502 (in Chinese)
[20] Hua X D, Wang W and Wang H 2016 *Acta Phys. Sin.* **65** 084503 (in Chinese)
[21] Zhang W H, Yan R, Feng Z X, Wang K 2016 *Acta Phys. Sin.* **65** 064501 (in Chinese)
[22] Vicsek T, Czirók A, Ben-Jacob E, Cohen I and Shochet O 1995 *Phys. Rev. Lett.* **75** 1226
[23] Barberis L and Peruani F 2016 *Phys. Rev. Lett.* **117** 248001
[24] Chowdhury D, Guttal V, Nishinari K and Schadschneider A 2002 *J. Phys. A* **35** L573
[25] Kunwar A, John A, Nishinari K, Schadschneider A and Chowdhury D 2004 *J. Phys. Soc. Jpn.* **73** 2979
[26] John A, Schadschneider A, Chowdhury D and Nishinari K 2009 *Phys. Rev. Lett.* **102** 108001
[27] Jiang R, Hu M B, Wu Q S and Song W G 2017 *Transp. Sci.* **51** 998
[28] Jiang R, Hu M B, Zhang H M, Gao Z Y, Jia B and Wu Q S 2015 *Transp. Res. B* **80** 338
[29] Tian B, Jiang R, Hu M B and Jia B 2017 *Chin. Phys. B* **26** 020503
[30] Guo N, Chen J Y, Hu M B and Jiang R 2016 *Chin. Phys. B* **25** 060505
[31] Ling X, Hu M B, Long J C, Ding J X and Shi Q 2013 *Chin. Phys. B* **22** 018904
[32] Suematsu N J, Nakata S, Awazu A and Nishimori H 2010 *Phys. Rev. E* **81** 056210
[33] Heisler E, Suematsu N J, Awazu A and Nishimori H 2012 *Phys. Rev. E* **85** 055201
[34] Chaudhuri D, Nagar A 2015 *Phys. Rev. E* **91** 012706
[35] Dussutour A, Fourcassie V, Helbing D and Deneubourg J L 2004 *Nature* **428** 70
[36] Dussutour A, Deneubourg J L and Fourcassié V D 2005 *Journal of Experimental Biology* **208** 2903
[37] Couzin I D and Franks N R 2003 *Proc. Roy. Soc. London B* **270** 139
[38] Fourcassié V, Dussutour A and Deneubourg J L 2010 *Journal of Experimental Biology* **213** 2357
[39] Li H and Zhang H P 2013 *Europhys. Lett.* **102** 50007
[40] http://www.hexbug.com/nano/